



Interstitial telomeric sequences promote gross chromosomal rearrangement via multiple mechanisms

Fernando R. Rosas Bringas^{a,1} , Ziqing Yin^{a,1} , Yue Yao^a , Jonathan Boudeman^a, Sandra Ollivaud^{a,1} , and Michael Chang^{a,2}

Edited by Richard Kolodner, Ludwig Institute for Cancer Research Ltd., La Jolla, CA; received April 11, 2024; accepted October 10, 2024

Telomeric DNA sequences are difficult to replicate. Replication forks frequently pause or stall at telomeres, which can lead to telomere truncation and dysfunction. In addition to being at chromosome ends, telomere repeats are also present at internal locations within chromosomes, known as interstitial telomeric sequences (ITSs). These sequences are unstable and prone to triggering gross chromosomal rearrangements (GCRs). In this study, we quantitatively examined the effect of ITSs on the GCR rate in *Saccharomyces cerevisiae* using a genetic assay. We find that the GCR rate increases exponentially with ITS length. This increase can be attributed to the telomere repeat binding protein Rap1 impeding DNA replication and a bias of repairing DNA breaks at or distal to the ITS via de novo telomere addition. Additionally, we performed a genome-wide screen for genes that modulate the rate of ITS-induced GCRs. We find that mutation of core components of the DNA replication machinery leads to an increase in GCRs, but many mutants known to increase the GCR rate in the absence of an ITS do not significantly affect the GCR rate when an ITS is present. We also identified genes that promote the formation of ITS-induced GCRs, including genes with roles in telomere maintenance, nucleotide excision repair, and transcription. Our work thus uncovers multiple mechanisms by which an ITS promotes GCR.

interstitial telomeric sequence | gross chromosomal rearrangement | de novo telomere addition | telomeric DNA replication | DNA repair

Telomeres consist of repetitive DNA sequences and associated proteins and are essential structures that “cap” and protect the ends of eukaryotic chromosomes (1). A dysfunctional telomere will cause the chromosome end to be recognized as DNA damage, activating the DNA damage response and inhibiting cell proliferation. Telomeres, however, are also problematic because they are difficult to replicate. First, due to the enzymatic characteristics of DNA polymerases, the standard DNA replication machinery cannot fully replicate DNA ends—a problem famously referred to as the end replication problem (2). This problem is solved by an enzyme called telomerase, which adds telomeric repeats to the ends of the chromosomes (3). A second (and less-appreciated) problem is that DNA replication forks often stall and collapse while traversing telomeric sequences. This is highly conserved throughout evolution, having been reported in budding yeast *Saccharomyces cerevisiae*, fission yeast *Schizosaccharomyces pombe*, and mouse and human cells (4–7).

There are at least three obstacles that could hinder the progression of the replication fork through telomeric sequences: 1) proteins that are tightly bound to telomeric sequences; 2) secondary structures (e.g., G-quadruplexes) that form due to the repetitive G-rich nature of telomeres (8); and 3) RNA-DNA hybrids formed from the transcription of telomeric repeat-containing RNA (TERRA; 9). If such impediments to replication fork progression are not properly dealt with, telomeres can become truncated and dysfunctional.

The difficulty of replicating telomeric repeats extends to telomeric sequences located at internal regions of the genome, called interstitial telomeric sequences (ITSs). ITSs are naturally found in the genomes of many species and are thought to be either remnants of ancestral chromosomal fusions or erroneous insertions of telomeric repeats that occur during the repair of DNA double-strand breaks (DSBs; 10, 11). The human genome contains over 80 ITSs that have at least four telomeric repeats (12). Stalling of DNA replication at ITSs has been well documented in *S. cerevisiae*, both in vivo (5, 13, 14) and in vitro (15). ITSs are especially hazardous to genome stability because they are prone to breakage, provoke genome rearrangements, and are often found at translocation break-points in cancer cells (11, 16, 17). A break at an ITS can also be “healed” by telomerase, resulting in the generation of a new telomere and loss of genetic material distal to the ITS. Such de novo telomere addition events have been linked to human disorders, including terminal deletions of chromosome 16 (alpha-thalassemia; 18, 19) and chromosome 12 (mental retardation; 20).

Significance

Telomeric DNA repeats are found at the ends of linear chromosomes where they, together with specialized proteins that bind to them, protect chromosome ends from degradation and unwanted DNA repair activities. Telomeric repeats can also be found at internal locations in the genome, where they are called interstitial telomeric sequences (ITSs). ITSs are prone to breakage and are associated with human diseases. In this study, using baker's yeast as a model organism, we show that instability at ITSs is driven by multiple factors and identify genes that either promote or suppress gross chromosomal rearrangements induced by the presence of an ITS.

Author affiliations: ^aEuropean Research Institute for the Biology of Ageing, University of Groningen, University Medical Center Groningen, Groningen 9713 AV, The Netherlands

Author contributions: F.R.R.B. and M.C. designed research; F.R.R.B., Z.Y., Y.Y., J.B., and S.O. performed research; F.R.R.B., Z.Y., Y.Y., J.B., S.O., and M.C. analyzed data; and F.R.R.B. and M.C. wrote the paper.

The authors declare no competing interest.

This article is a PNAS Direct Submission.

Copyright © 2024 the Author(s). Published by PNAS. This open access article is distributed under Creative Commons Attribution License 4.0 (CC BY).

¹F.R.R.B. and Z.Y. contributed equally to this work.

²To whom correspondence may be addressed. Email: m.chang@umcg.nl.

This article contains supporting information online at <https://www.pnas.org/lookup/suppl/doi:10.1073/pnas.2407314121/-/DCSupplemental>.

Published November 27, 2024.

In this study, we quantitatively measured ITS stability in *S. cerevisiae* using a gross chromosomal rearrangement (GCR) assay. We find that GCR rates rise exponentially with increasing ITS length. This increase is caused by the presence of the telomere repeat binding protein Rap1, which is known to impede DNA replication (5, 14, 15, 21), and a strong preference for repairing DNA breaks at or distal to the ITS by de novo telomere addition. In addition, we performed a genome-wide screen to identify genes that contribute to ITS stability. We find that mutations in DNA replication genes elevate GCR rates, but many genes reported as general GCR suppressors do not exhibit an effect in the presence of an ITS. We also identified genes that promote ITS-induced GCRs, including genes important for telomere maintenance, nucleotide excision repair, and transcription. Our work reveals the multiple mechanisms by which an ITS promotes GCR.

Results

The GCR Rate Increases Exponentially with ITS Length. To quantitatively assess ITS stability, we modified the GCR assay developed by Chen and Kolodner by inserting an ITS of varying lengths between the most telomere-proximal essential gene on the left arm of chromosome V (*PCMI*) and two counterselectable markers (*CAN1* and *URA3*) used in the original assay (22; Fig. 1A). The GCR rate (GCR events per cell division) can be determined by measuring the rate of simultaneous loss of *CAN1* and *URA3*—detected by growth on canavanine and 5-fluoroorotic acid (5-FOA), respectively—with a fluctuation test. We observe that the GCR rate increases with ITS length in two distinct exponential phases (Fig. 1B and *SI Appendix*, Fig. S1 and Table S1). Up to 50 bp, the GCR rate increases rapidly (1.6×10^{-9} with no ITS to 4.5×10^{-6} with a 50-bp ITS); beyond 50 bp, the GCR rate still increases exponentially, but more modestly (to 1.5×10^{-4} with a 300-bp ITS). To rule out the possibility that the increase in the GCR rate is simply due to the high G/C content of the ITS, we inserted 300 bp of lambda phage DNA, which has a 62% G/C content, similar to wild-type telomeric sequence. The GCR rate of this strain is similar to that of the “no-ITS” control (Fig. 1C and *SI Appendix*, Table S1). Telomeric sequences promote transcriptional silencing of adjacent genes (23). To determine whether the increase in the GCR rate was in part caused by silencing of the *CAN1* and *URA3* genes, we measured the GCR rate in a 300-bp ITS-containing strain deleted for *SIR2*, a gene needed for silencing (24). We find that the absence of Sir2 does not affect the GCR rate (Fig. 1C and *SI Appendix*, Table S1). Thus, the ITS-induced increase in the GCR rate is due neither to the high G/C content of the ITS nor to silencing of the GCR markers.

Two main factors can explain why the GCR rate increases with ITS length. First, telomeric DNA is difficult to replicate, so the longer the ITS, the greater the possibility for a GCR event to occur. Second, if a DNA break occurs at or distal to the ITS, the probability that the break is “repaired” by de novo telomere addition (resulting in a GCR) is very high if at least 34 bp of telomeric sequence is present on the centromere side of the break. A sharp threshold separates a DSB from a telomere; DNA ends with 34 bp of telomeric sequence are recognized as critically short telomeres and efficiently extended by telomerase, whereas those with less than 34 bp are not (25). The bias toward repair via de novo telomere addition reaches a maximum once the ITS is sufficiently longer than this threshold; once a DNA end looks like a telomere, it cannot look even more like a telomere—at least in terms of de novo telomere addition. Thus, the increase in the GCR rate is more modest once the ITS is longer than 50 bp.

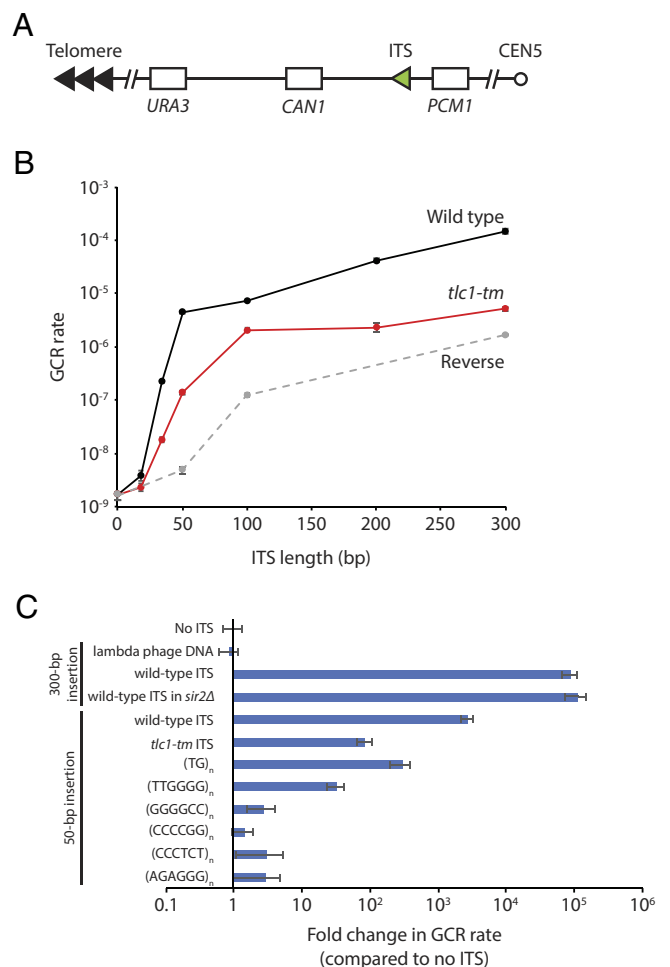


Fig. 1. The GCR rate increases with ITS length due to Rap1-dependent inhibition of replication and a bias of repairing DNA breaks via de novo telomere addition. (A) Schematic diagram of the ITS-GCR assay. Loss of both *URA3* and *CAN1* allows growth on 5-FOA and canavanine. ITSs of varying lengths were inserted between *CAN1* and *PCMI*, the most telomere-proximal essential gene on the left arm of chromosome V. (B) GCR rate plotted as a function of ITS length. Wild-type ITS in black; *tlc1-tm* ITS in red; reverse orientation ITS in dashed gray. (C) GCR rates of strains with the indicated sequence insertions are plotted. Error bars in (B and C) represent SEM (n = 3 or 4).

Note that the inflection point does not occur at 34 bp because a break could occur either within the ITS or distal to the ITS. For a 34-bp ITS, the break that leads to the de novo telomere addition most likely occurs distal to the ITS; if it were to occur within the ITS, the resulting DNA end would have less than 34 bp of telomeric sequence and would therefore not be efficiently extended by telomerase. For increasingly longer ITSs, the probability that the break occurs within the ITS increases, as does the probability of that break leaving at least 34 bp of telomeric sequence on the centromere side of the break. Both of these probabilities will eventually reach a maximum (i.e., at a certain ITS length, almost all breaks will occur within the ITS, and almost all of these breaks will leave at least 34 bp of telomeric sequence on the centromere side of the break), and further increases in ITS length will not affect these factors (although the GCR rate will continue to increase due to Rap1-mediated fork collapse; see below). We do not know the exact ITS length where this effect occurs, but the net effect is an inflection point in the GCR rate curve at approximately 50 bp in ITS length.

Rap1 Contributes to the ITS-Induced Increase in the GCR Rate. The difficulty in replicating telomeric DNA has been attributed to the binding of Rap1 to telomeric repeats (5, 14, 15, 21). To

test whether Rap1 is promoting the ITS-induced increase in the GCR rate, we examined the effect of an ITS with *tlc1-tm* [(TG)₀₋₄TGG]_nATTTGG telomeric repeats (26), rather than wild-type (TG)₀₋₆TGGGTGTG(G)₀₋₁ repeats (27). The *tlc1-tm* mutant repeats disrupt Rap1 association, but can still be efficiently recognized by telomerase and cap telomeres when located at chromosome ends (28). We find that the *tlc1-tm* ITS also increases the GCR rate, but to a lesser extent than the wild-type ITS (Fig. 1B and *SI Appendix, Table S1*). The relationship between the GCR rate and *tlc1-tm* ITS length is consistent with the DSB-telomere threshold, which is not affected by Rap1 binding (25), playing a dominant role. As *tlc1-tm* ITS length increases, repair by de novo telomere addition increases, reaching a maximum once the *tlc1-tm* ITS is sufficiently longer than the DSB-telomere threshold. However, the more modest exponential increase in the GCR rate observed with wild-type ITS lengths above 50 bp is not seen with the *tlc1-tm* ITS, suggesting that this increase is promoted by Rap1. Since Rap1 is not completely depleted from *tlc1-tm* sequences (28), we also measured the effect of a 50-bp insertion of TG dinucleotides, i.e., (TG)₂₅, which is predicted to disrupt Rap1 binding even more so than *tlc1-tm* repeats (29), but like *tlc1-tm*, can still be efficiently extended by telomerase (25). We find that the (TG)₂₅-induced GCR rate is comparable to the 50-bp *tlc1-tm* ITS-induced GCR rate; i.e., there is an increase in the GCR rate, but much less than with a 50-bp wild-type ITS (Fig. 1C and *SI Appendix, Table S2*). The difficulty in replicating telomeric sequences has also been attributed to the formation of G-quadruplexes, which is compromised in TG dinucleotide and *tlc1-tm* repeats (30). Thus, we also tested 50 bp of TTGGGG *Tetrahymena* telomeric repeats, which can be extended by *S. cerevisiae* telomerase (31) and have the ability to form G-quadruplexes (32), but does not bind Rap1 (33). We find that this sequence increases the GCR rate to a level slightly less than that of the 50-bp *tlc1-tm* ITS (Fig. 1C and *SI Appendix, Table S2*). These findings suggest that Rap1, rather than G-quadruplex formation, promotes the wild-type ITS-induced increase in the GCR rate.

To further assess the ability of G-quadruplexes to induce GCR, we measured the effect of inserting 50 bp of the hexanucleotide repeats GGGGCC/GGCCCC and CCCTCT/AGAGGG on the GCR rate. Expansion of these repeats cause neurodegenerative diseases (amyotrophic lateral sclerosis and frontotemporal degeneration for GGGGCC/GGCCCC and X-linked dystonia parkinsonism for CCCTCT/AGAGGG), and the formation of G-quadruplexes by these repeats has been proposed to be involved in their expansion (34). The insertion of these sequences only mildly increases the GCR rate (Fig. 1C and *SI Appendix, Table S2*). Our findings indicate that G-quadruplexes play a relatively minor role, in comparison to Rap1, in hindering the replication of *S. cerevisiae* telomeric DNA, in agreement with previous work, including an in vitro study examining the replication of telomeric sequences with and without Rap1 (5, 15).

Interestingly, while 50-bp insertions of *tlc1-tm* repeats, (TG)_n repeats, and (TTGGGG)_n repeats are all i) deficient in Rap1 binding, ii) able to seed the formation of a de novo telomere, and iii) have reduced GCR rates compared to a 50-bp wild-type ITS, their GCR rates range from 5.2×10^{-8} for (TTGGGG)_n (~30-fold higher than the no-ITS control) to 4.8×10^{-7} for (TG)_n (~300-fold higher than the no-ITS control). The higher GCR rate caused by (TG)₂₅ could be due its ability to form Z-DNA (35).

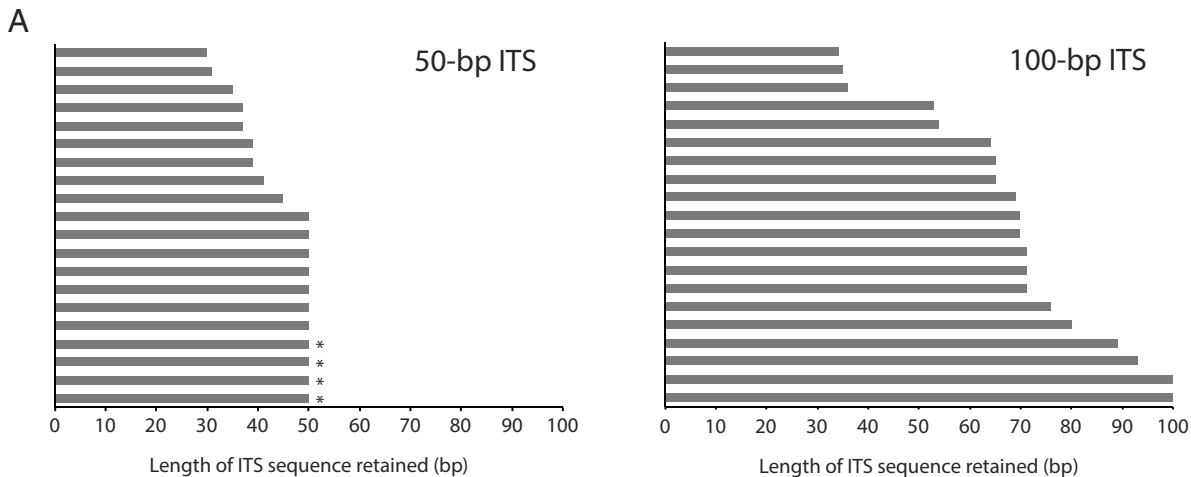
Breaks Occur within and Distal to the ITS. Since most GCR events detected in this assay without an ITS are predominantly de novo telomere addition events (36), we reasoned that the addition of an ITS would only further increase this bias, most

likely with the new telomere added at the ITS. Thus, to gain insight into the mechanisms that underlie the increased GCR rates induced by the presence of an ITS, we sequenced the ITS region from independently isolated canavanine- and 5-FOA-resistant mutants (i.e., GCR survivors) derived from strains that either had the 50-bp ITS or the 100-bp ITS, 20 from each strain. As we expected, de novo telomere addition occurred at the ITS in all 40 GCR survivors. Since yeast telomerase adds imperfect, degenerate repeats (27), we can determine the exact position where telomerase added the new telomere by comparing with the original 50-bp and 100-bp ITSs (Fig. 2A). Only a centromere-proximal portion of the ITS was retained in some of the GCR survivors (nine of 20 derived from the 50-bp ITS strain, 18 of 20 derived from the 100-bp ITS strain), suggesting that the DNA replication fork collapsed while traversing the ITS, followed by the telomerase-mediated addition of a new telomere. In all GCR survivors, at least 30 bp of the original ITS was retained, consistent with DNA ends with less than 30 bp of telomeric sequence being recognized as DSBs and not efficiently extended by telomerase (25).

Surprisingly, the entire ITS was retained in the remaining GCR survivors (11 of 20 derived from the 50-bp ITS strain, two of 20 derived from the 100-bp ITS strain). These findings suggest that the DNA replication fork likely collapsed distal to the ITS, followed by resection back to the ITS prior to telomere addition, leaving the original ITS intact. Consistent with our observations, it has been previously shown that sites of repair-associated telomere addition (SiRTAs; hot spots in the genome for de novo telomere addition) can be located several kilobases away from an induced DSB (37). In four GCR survivors derived from the 50-bp ITS strain, up to 10 bp immediately downstream of the ITS was also retained (Fig. 2B). This is analogous to SiRTAs, which have a bipartite structure consisting of a Stim sequence and a Core sequence; Cdc13 can bind to a Stim sequence (in this case, the ITS) and stimulate de novo telomere addition at the downstream Core sequence (37).

For the GCR survivors that only retained a part of the original ITS, it is formally possible that breaks occurred distal to the ITS (rather than within the ITS), followed by resection into the ITS before telomere addition. However, resection of telomeric sequence is expected to be limited by Cdc13 (38, 39). Consistent with limited resection, when we sequenced 21 independent isolates of de novo telomeres generated by making an HO endonuclease cut immediately adjacent to 82 bp of telomeric sequence, only up to 3 bp of the original 82-bp seed sequence was lost (7 of 21 isolates); the majority of the isolates (14 of 21 isolates) had retained all 82 bp (*SI Appendix, Fig. S2*).

Reversing the Orientation of the ITS. In the above experiments, the orientation of the ITS is the same as the telomere of the chromosome arm (V-L) on which it is located. Reversing the orientation of the ITS should reduce the GCR rate because the ITS cannot seed the formation of a new telomere in the correct orientation. Consistent with this hypothesis, this is indeed what we observe (Fig. 1B and *SI Appendix, Table S1*). The GCR rate still increases exponentially, likely due to Rap1-dependent stalling of replication fork progression, which has previously been shown to be orientation independent (5, 21; although a difference in the magnitude of the stall was reported in ref. 13), leading to other types of GCR that do not arise from the addition of a new telomere using the ITS as a seed sequence. Our data are seemingly at odds with those from a previous study showing that an ITS with the C-rich sequence serving as the lagging strand template (i.e., the reverse orientation) results in expansion of telomeric repeats rather than GCR (40). There are several important features



B

```

50.ref  ...TGTGTGTGGGTGTGGGTGTGAATTCAGTGGCCGTCGTTTTACAACGTCAGTGGCCTATGCGGCCGCGGATCTGCCGG...
50.2    ...TGTGTGTGGGTGTGGGTGTGAATTCAGTGGTGTGGGTGTGGTGTGTGGGTGTGGGTGTGTGGGTGTGGTGTGGGTGTG...
50.4    ...TGTGTGTGGGTGTGGGTGTGAATGGGTGTGGGTGTGGGTGTGGTGTGTGGGTGTGGTGTGTGGGTGTGGTGTGGGTGTG...
50.11   ...TGTGTGTGGGTGTGGGTGTGAATTCAGTGGTGTGGGTGTGGTGTGTGGGTGTGGGTGTGTGGGTGTGGTGTGTGGGTGTG...
50.21   ...TGTGTGTGGGTGTGGGTGTGAATTCAGTGGTGGGTGTGTGGGTGTGTGGGTGTGGTGTGGGTGTGGTGTGTGGGTGTGG...

```

Fig. 2. Breaks occur within and distal to the ITS. (A) GCR survivors were isolated by growing strains with either a 50-bp ITS or 100-bp ITS on agar plates containing canavanine and 5-FOA. Twenty independent isolates from each strain were analyzed. In all 40 isolates, the presence of a de novo telomere added at the ITS site was confirmed by PCR and sequencing. The length of the original ITS retained for each de novo telomere is plotted. Four isolates also retained sequence downstream of the ITS and are indicated by an asterisk. (B) The sequences of the four isolates are aligned to DNA sequence from the original 50-bp ITS-containing strain (50.ref). The last 20 bp of the ITS are underlined. Newly added telomeric sequence in the GCR survivors is in bold and red.

in the assay used in the previous study that likely explain this difference. First, the ITS was located within an intron and thus was transcribed. Second, the assay does not specifically select for GCRs, so an increase in the GCR rate may have been masked by a much larger increase in expansion events. Last, the ITS consisted of eight identical repeats of the CCCACACA sequence (reverse complement: TGTGTGGG). Native yeast telomeric sequence consists of imperfect (TG)₀₋₆TGGGTGTG(G)₀₋₁ repeats (27), and it is known that imperfections in repetitive sequences decrease the rate of repeat expansion (34).

Identification of Genes That Suppress ITS-Induced GCR Events.

To identify genes that suppress ITS instability, we used a high-throughput replica-pinning approach that we recently developed to detect low-frequency events (41), such as GCRs. First, we introduced the 50-bp ITS GCR assay components into the yeast knockout (YKO) and conditional temperature-sensitive (ts) strain libraries (42, 43) using the synthetic genetic array (SGA) method (44). The resulting strains were amplified by high-throughput replica-pinning, yielding 24 colonies per YKO or ts strain, onto media containing canavanine and 5-FOA to select for GCR events (see *Materials and Methods* for details). GCR frequencies (percentage of GCR-positive colonies) were calculated for each mutant strain (Fig. 3A). The median GCR frequency was 38% for the YKO strains and 42% for the ts strains. Only mutants with a GCR frequency above 70% (corresponding to a Fisher's exact test *P*-value of <0.002) were analyzed further (Dataset S1). A total of 54 YKO and 44 ts mutants met this criterion. These strains were generated again by SGA and further tested using a patch-and-replica-plate approach (Fig. 3B; 45), from which 21 mutants (5 YKO and 16 ts) appeared to have an increased ITS-induced GCR rate. Their GCR rates were determined by fluctuation tests. Ten of the 21 mutants have more than a twofold increase in ITS-induced GCR rate (Fig. 3C and *SI Appendix, Table S3*). It should be noted

that the high GCR rate caused by the 50-bp ITS (~2,750-fold increase) may make it difficult to identify mutants that further increase the GCR rate, given that even strong GCR mutators, such as *pif1Δ* and *rad27Δ*, only exhibit a ~1,000-fold increase in the GCR rate in the absence of an ITS (46). Thus, the identification of these 10 mutants despite this potential technical obstacle may suggest that they cause ITS-specific increases in the GCR rate, in addition to any general (i.e., non-ITS-specific) effects on the GCR rate they may have.

Of these nine genes (two of the mutants are different alleles of *CDC2*), eight are primarily involved in DNA replication (*CDC2/POL3*, *CDC9*, *ELG1*, *RAD27*, *RFC2*, *RFC4*, *RFC5*, and *YDL162c*). Pol3 is the catalytic subunit of DNA polymerase δ (47, 48). Rfc2, Rfc4, and Rfc5 are small subunits of the replication factor C (RFC) complex, which catalyzes the loading of the proliferating cell nuclear antigen (PCNA) sliding clamp (49). Elg1 forms an alternative RFC complex with Rfc2–5 that is implicated in unloading PCNA (50). Rad27 is a flap endonuclease involved in Okazaki fragment processing and maturation (51). Cdc9 is DNA ligase I, responsible for ligating Okazaki fragments together (52). *YDL162c* is an open reading frame that overlaps with the *CDC9* promoter; its deletion reduces *CDC9* expression (53). The ninth gene, *RPT4*, encodes an ATPase of the 19S regulatory particle of the 26S proteasome (54), which is important for many cellular functions, including DNA replication and genome stability (55).

With the exception of *RPT4*, all of these genes also suppress the GCR rate in the absence of an ITS (Fig. 3C and *SI Appendix, Table S3*), which is not surprising given that these genes are involved in DNA replication; defects in DNA replication should increase GCRs regardless of whether an ITS is present. The ITS-specific increase in the GCR rate observed in the *rpt4-150* strain may indicate that the proteasome removes a GCR-inducing protein that is bound to the ITS. An obvious candidate for such a protein is Rap1, although we do not detect a change in cellular

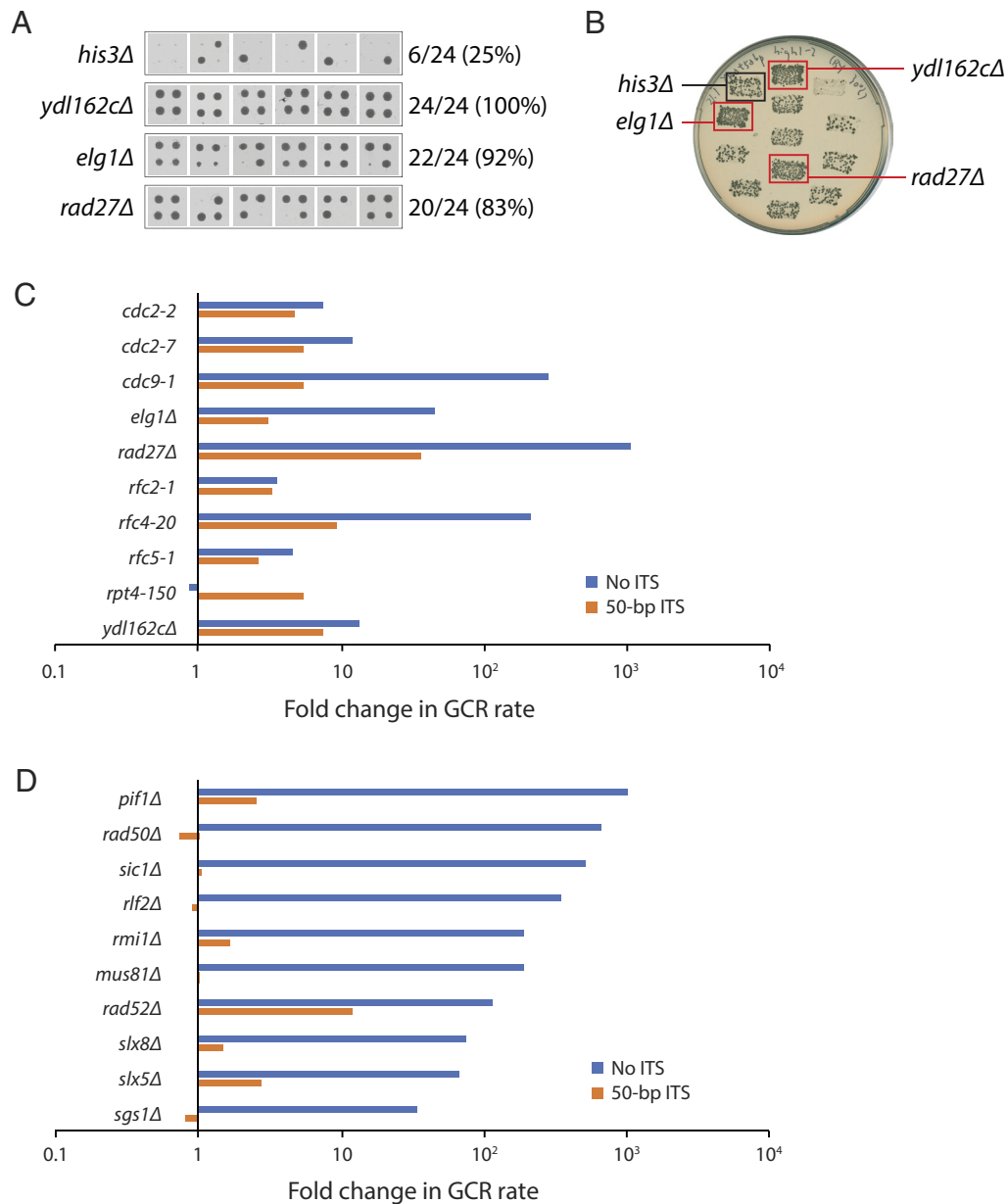


Fig. 3. Identification of genes that suppress the ITS-induced GCR rate. (A) A high-throughput screen was performed as described in the text. All 24 replica-pinned colonies on media containing both canavanine and 5-FOA of the *his3Δ* control strain and three selected mutants with increased GCR frequencies are shown. (B) Putative hits from the high-throughput screen were tested in a patch-and-replica-plate assay. An example plate, with three mutants that tested positive (red boxes), is shown. A negative control (*his3Δ*) and a positive control (*ydl162cΔ*) were included on each plate. (C) Fold change in the GCR rate of mutants identified in the ITS-GCR screen. (D) Fold change in the GCR rate of 10 known GCR suppressors not identified in the ITS-GCR screen. (C and D) Fold change of mutants without an ITS is relative to a wild-type strain without an ITS. Fold change of mutants with a 50-bp ITS is relative to a wild-type strain with an ITS. Note that plotting fold changes in this manner obscures the large difference in the GCR rates without and with an ITS. Raw values for the GCR rate can be found in [SI Appendix, Tables S3 and S4](#). Data for YKO strains without an ITS were taken from a previous publication (46).

Rap1 levels in *rpt4-150* cells ([SI Appendix, Fig. S3](#)). However, other explanations for the ITS-specific effect of *rpt4-150* are possible, and further studies are necessary to elucidate the mechanism.

Many Mutants Increase the GCR Rate in the Absence of an ITS but Not in Its Presence. Many mutants have been reported to increase the GCR rate in the absence of an ITS (46, 56). Interestingly, the majority of these mutants were not identified in our screen and might be false negatives. Therefore, we measured the GCR rate of 10 of these mutants in the presence of a 50-bp ITS (Fig. 3D and [SI Appendix, Table S4](#)). Seven of these mutants do not significantly alter the ITS-induced GCR rate (i.e., less than 1.7-fold; *rad50Δ*, *sic1Δ*, *rlf2Δ*, *rmi1Δ*, *mus81Δ*, *slx8Δ*, and *sgs1Δ*). For the remaining three, *pif1Δ*, *rad52Δ*, and *slx5Δ* increase the ITS-induced GCR rate

by 2.5-, 12-, and 2.7-fold, respectively, far lower than their effect on the GCR rate in the absence of an ITS. Thus, it appears that many known GCR suppressors have a greatly reduced, if not completely absent, role in suppressing GCRs when an ITS is present. We also tested *rrm3Δ* because Rrm3 is a helicase that promotes replication fork progression through telomeric sequences (4). Deletion of *RRM3* has been reported to exhibit a mild fourfold increase in the GCR rate in the absence of an ITS (57); we find that this is also true in the presence of an ITS ([SI Appendix, Table S4](#)). Since the ITS-induced GCR rate is increased in *rad52Δ* cells, and Rad52 is important for all homology-dependent processes, we tested the loss of *RAD51* and *POL32*, two genes that also have roles in these processes (58); neither increases the ITS-induced GCR rate ([SI Appendix, Table S4](#)).

Most known GCR suppressors have roles in DNA replication or repair. However, one exception that stands out is the cyclin-dependent kinase inhibitor Sic1. Cells lacking Sic1 initiate DNA replication from fewer origins of replication, causing an increase in the distance a replication fork has to travel and in the time needed to replicate the entire genome (59), including the region of chromosome V relevant for the GCR assay (60). It was suggested that ongoing replication as *sic1Δ* cells enter anaphase may lead to an increase in DSBs and GCRs (59). ITS-induced pausing of the replication fork would also cause a delay in replicating DNA distal to the ITS, resulting in underreplication and DNA breaks distal to the ITS, consistent with the data we obtained by sequencing GCR survivors (Fig. 2). The lack of an increase in the GCR rate in *sic1Δ* strains with a 50-bp ITS suggests that the ITS is epistatic to *sic1Δ* in terms of delaying replication of the left arm of chromosome V. In other words, replication of the chromosomal region distal to the ITS is chronically delayed, so much so that further deletion of *SIC1* cannot make it worse.

The *rfc2-1* and *rfc5-1* Mutations Dramatically Accelerate Senescence in the Absence of Telomerase. Mutations that increase the ITS-induced GCR rate likely increase the probability of replication fork collapse within the ITS. Such mutations may also increase fork collapse at native telomeres, which could lead to truncation of telomeres and accelerated senescence in the absence of telomerase. Consistent with this idea, *cdc2-2* and *rad27Δ* have both been reported to cause accelerated senescence in the absence of telomerase (61, 62). We tested the remaining eight mutations that increase the ITS-induced GCR rate. We sporulated diploids that are heterozygous in one of the genes of interest as well as *EST2*, which encodes the protein catalytic subunit of telomerase (63), and followed the growth of the haploid meiotic progeny by serial propagation in liquid cultures for several days (Fig. 4). As expected, *est2Δ* cultures grew slower as the experiment progressed and cells senesced, but growth was eventually restored upon the emergence of survivors that utilize recombination-mediated mechanisms to maintain telomeres (64). We find that *est2Δ rfc2-1* and *est2Δ rfc5-1* double mutants senesce much faster than *est2Δ* single mutants. The *cdc2-7*, *cdc9-1*, and *elg1Δ* mutations appear to modestly accelerate senescence, while the *rpt4-150* mutation causes a slight delay in senescence. Thus, seven of the 10 mutants found to elevate the ITS-induced GCR rate also cause accelerated senescence in the absence of telomerase.

Identification of Mutants That Decrease the ITS-Induced GCR Rate. We repeated the genome-wide screen with minor adjustments that allowed us to identify mutants that decrease the ITS-induced GCR rate (see *Materials and Methods* for details). The median GCR frequency was 79% for the YKO strains and 67% for the ts strains. Only mutants with a GCR frequency below 38% for the YKO strains and 31% for the ts strains (corresponding to a Fisher's exact test P -value of $<10^{-4}$) were analyzed further (Fig. 5A and Dataset S2). A total of 248 YKO and 114 ts mutants met this criterion. These strains were generated again by SGA and further tested using the patch-and-replica-plate approach (Fig. 5B). A large number of the remaining genes have roles in chromosome segregation, spindle assembly checkpoint, and microtubule-based processes. The identification of these genes is due to the *CIN8* gene located distal to the ITS on chromosome V (65). De novo telomere addition at the ITS results in the loss of *CIN8*, which is synthetic lethal with mutation of these genes. Thus, we eliminated the hits that are known to be synthetic lethal with *cin8Δ*. We also retested these mutants with the patch-and-replicate-plate approach after

introducing an extra copy of *CIN8* located elsewhere in the genome and eliminated hits that did not show a decrease in ITS-induced GCRs. Finally, we performed an SGA analysis of the hits, identifying and eliminating those that showed a negative synthetic genetic interaction with truncation of chromosome V at the ITS. The remaining 180 (122 YKO and 58 ts) hits show a high degree of enrichment for genes involved in nucleotide excision repair and transcription (Fig. 5C and *SI Appendix, Table S5*). A subset of the mutants was subjected to fluctuation tests to determine their ITS-induced GCR rates (Fig. 5D and *SI Appendix, Tables S5 and S6*).

As expected, our screen identified *EST1*, *EST2*, and *EST3*, which encode the three protein subunits of telomerase (66). Deleting either *EST1*, *EST2*, or *EST3* has no significant effect on the GCR rate in the absence of an ITS (67). In contrast, in the presence of an ITS, deletion of *EST1*, *EST2*, or *EST3* decreases the GCR rate by approximately 300-fold. However, *est1Δ*, *est2Δ*, and *est3Δ* strains with a 50-bp ITS have GCR rates that are still fivefold higher than a wild-type strain without an ITS, indicating that a 50-bp ITS can induce the formation of GCRs that are not the result of telomerase-mediated de novo telomere addition. These GCRs are still likely triggered by Rap1-mediated inhibition of replication, causing breaks either within or distal to the ITS that are repaired in a manner that leads to other types of GCRs, such as nonreciprocal translocations or interstitial deletions.

The *cdc13-1* and *rap1-1* mutants exhibit 5.5- and 159-fold decreases, respectively, in the GCR rate in the presence of a 50-bp ITS. The *cdc13-1* result is consistent with our previous observation that this mutant is defective in generating a new telomere at a DNA end with 34 bp of telomeric sequence (25). Cdc13 binds to single-stranded telomeric DNA and is important for preventing excessive resection of telomere ends and for telomerase recruitment (38, 68). The *cdc13-1* allele is defective in the former function (38). It has been reported that defective resection promotes de novo telomere addition (69), so it is possible that excessive resection in the *cdc13-1* mutant impairs de novo telomere addition.

The *rap1-1* allele encodes a Rap1 mutant protein that has an amino acid change (A563P) in the DNA-binding domain (consisting of two Myb domains) and is compromised in binding DNA (70) and may therefore be less capable of obstructing DNA replication and inducing GCR. A563 is located in the central region of Rap1, and our finding is consistent with a previous study showing that the central region, which contains the two Myb domains and a transcription activation domain, is responsible for Rap1-mediated replication stalling and DSB induction (14). In contrast, neither the N-terminal region, which contains a BRCT domain, nor the C-terminal region, which is required for interactions with the Rif and Sir proteins (71–74), is needed for replication stalling and DSB induction (5, 14).

We also identified many genes (*RAD1*, *RAD2*, *RAD4*, *RAD10*, *RAD14*, *RAD23*, *RAD33*, and *TFB5*) required for nucleotide excision repair (NER). Deletion of *RAD1* and *RAD10* has previously been reported to reduce GCR formation in mutant strains with elevated GCR rates (75). Rad1 and Rad10 form a structure-dependent endonuclease that cleaves 3' flaps at junctions between single- and double-strand DNA during NER as well as homology-dependent repair processes (76). It was proposed that Rad1-Rad10 may cleave 3' flaps during the formation of a GCR, including the addition of a de novo telomere where the initiating break occurs distal to the addition site (75; *SI Appendix, Fig. S4A*). If this model is correct, the fraction of GCR survivors that retain the entire ITS should decrease in *rad1Δ* or *rad10Δ* mutants. However, we find that this is not the case (*SI Appendix, Fig. S4B*),

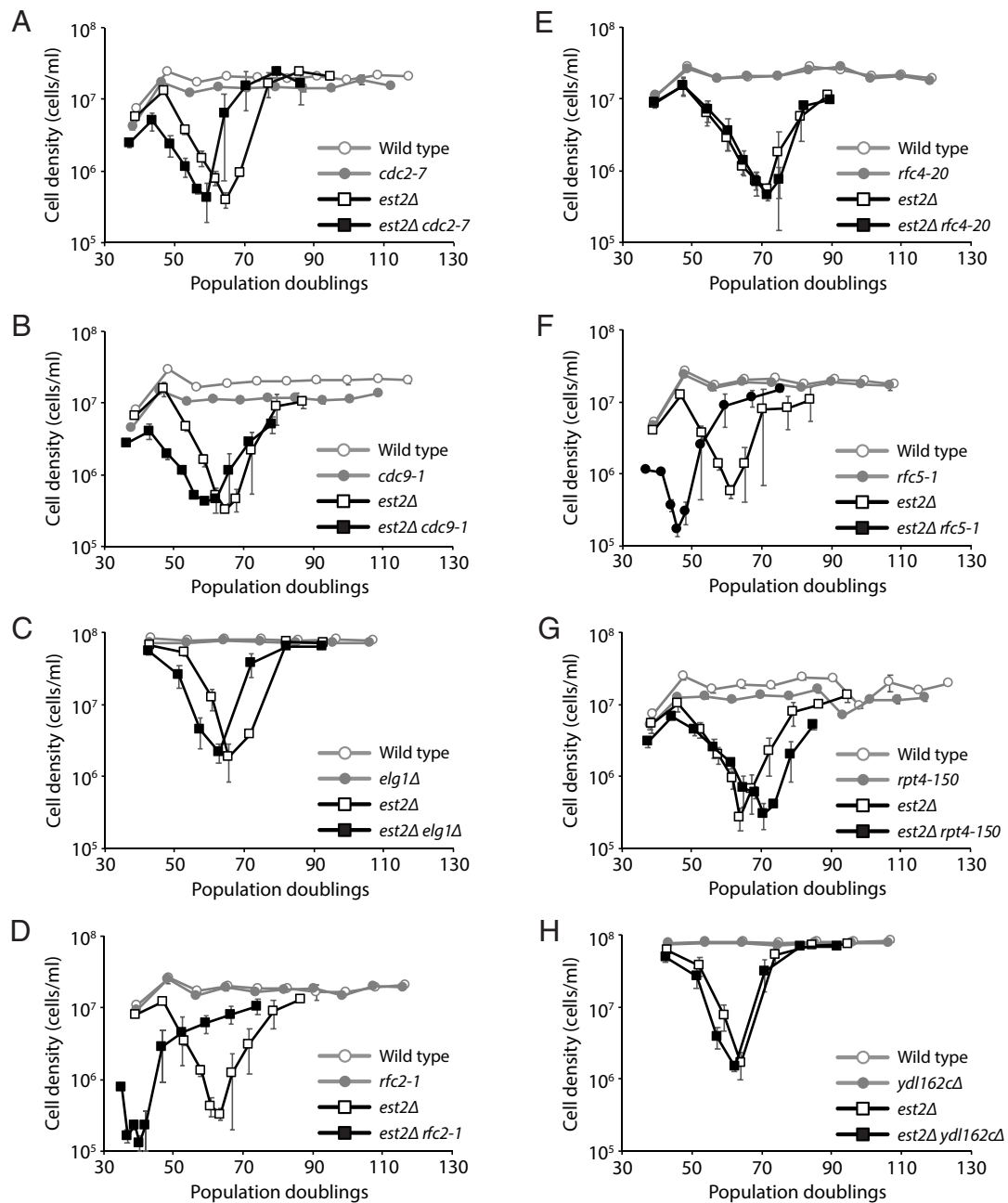


Fig. 4. The *cdc2-7*, *cdc9-1*, *elg1Δ*, *rfc2-1*, and *rfc5-1* mutations accelerate senescence in the absence of telomerase. Senescence was monitored by serial passaging of haploid meiotic progeny derived from the sporulation of ZYY238 (A), ZYY236 (B), ZYY232 (C), ZYY244 (D), ZYY246 (E), ZYY248 (F), ZYY240 (G), and ZYY228 (H). The average cell density \pm SEM of three independent isolates per genotype is plotted.

arguing against this model. Furthermore, the identification of many other genes involved in NER, which are not necessary for cleavage of 3' flap structures, suggests instead that Rad1-Rad10 promote GCR formation within the context of the NER pathway, at least in the presence of an ITS.

NER can be divided into two subpathways: global-genome NER (GG-NER) and transcription-coupled NER (TC-NER). The NER genes identified in the screen are important for both subpathways. In GG-NER, Rad7 and Rad16 form a stable complex that is needed for transcription-independent recognition of UV-induced damage, while Rad26 is involved in TC-NER (77). Deletion of *RAD7* or *RAD16* has no effect on the GCR rate, while deletion of *RAD26* decreases the GCR rate approximately threefold (SI Appendix, Table S6), suggesting the involvement

of TC-NER. It has been reported that R-loops, consisting of an RNA-DNA hybrid and displaced single-stranded DNA that can arise during transcription, are processed into DSBs by TC-NER (78). The identification of many genes with functions in transcription in our screen is consistent with R-loops promoting GCR via TC-NER. However, RNase H activity removes RNA-DNA hybrids, but cells lacking RNase H activity (*rnh1Δ rnh201Δ*) do not increase the ITS-induced GCR rate (SI Appendix, Table S7). Furthermore, the ITS-induced GCR rate is slightly increased, rather than decreased, upon overexpression of *RNH1* (SI Appendix, Table S8). Thus, R-loops are unlikely to promote ITS-induced GCR. Further studies are needed to elucidate the role of transcription and NER in promoting ITS-induced GCR.

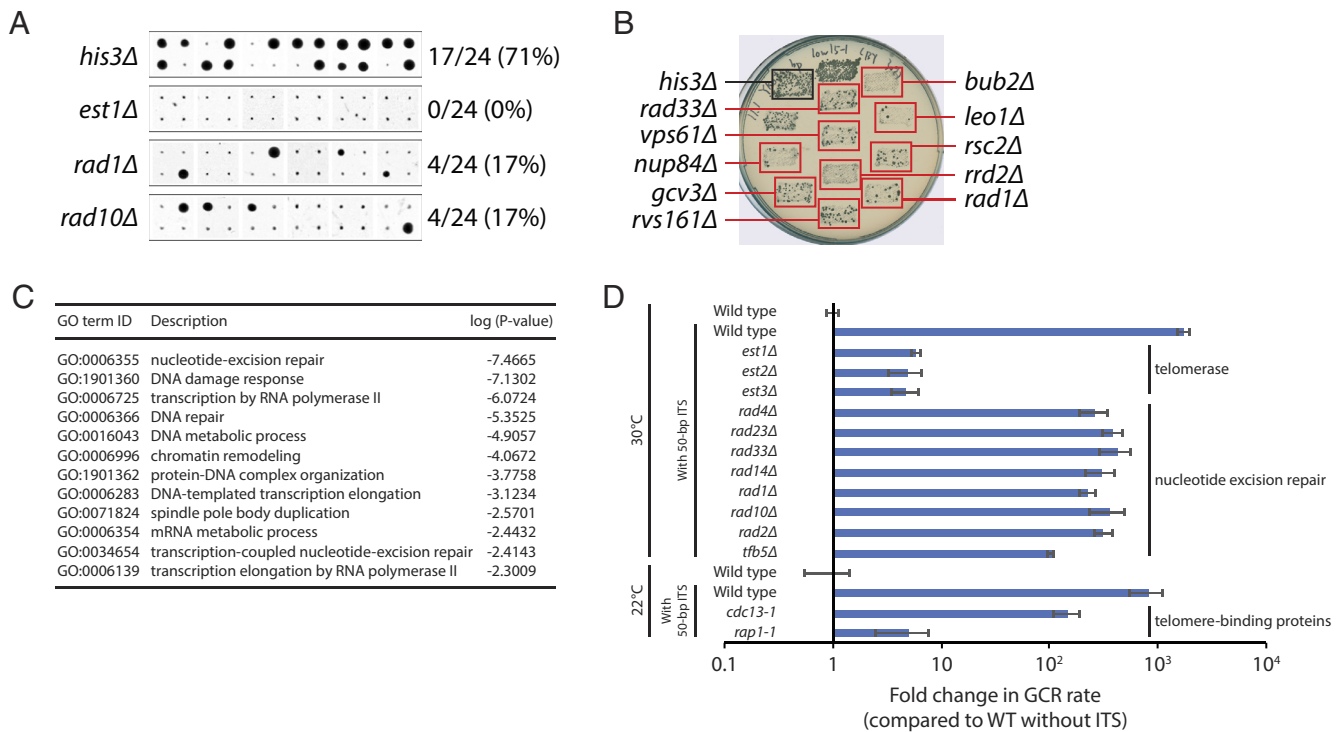


Fig. 5. Identification of genes that promote the ITS-induced GCR rate. (A) A high-throughput screen was performed as described in the text. All 24 replica-pinned colonies on media containing both canavanine and 5-FOA of the *his3Δ* control strain and three selected mutants with decreased GCR frequencies are shown. (B) Putative hits from the high-throughput screen were tested in a patch-and-replica-plate assay. An example plate, with 10 mutants that tested positive (red boxes), is shown. A negative control (*his3Δ*) and a positive control (*bub2Δ*) were included on each plate. (C) The statistically supported GO terms enriched in the genes that promote the ITS-induced GCR rate are shown. (D) GCR rates of the indicated strains containing a 50-bp ITS are plotted. Error bars represent SEM (n = 3 to 6).

Discussion

In this study, we examined ITS stability using a GCR assay in *S. cerevisiae*. We find that the GCR rate increases exponentially with ITS length, which can be attributed to Rap1-mediated inhibition of replication of telomeric sequence, and to a bias in repairing DNA breaks by de novo telomere addition. The latter effect maximizes once the ITS is approximately 50 bp in length, as the ITS becomes longer than the DSB-telomere transition length of 34 bp. In addition, we performed a genome-wide screen and identified nine genes that contribute to the stability of telomeric sequences, most of whom encode core components of the DNA replication machinery. Surprisingly, many genes previously reported to suppress GCRs in the absence of an ITS do not do so in the presence of an ITS, highlighting the ability of an ITS to override mechanisms that normally suppress GCRs. We also find that genes with roles in telomere maintenance, NER, and transcription can facilitate the formation of ITS-induced GCRs.

Binding of Rap1 to an ITS Promotes Its Instability. Our findings confirm and extend previous studies showing that DNA-bound Rap1, much more so than G-quadruplex formation, hinders replication fork progression through telomeric sequences and induces DNA breakage (5, 14, 15). We show that these breaks can occur within the ITS, but also distal to the ITS. The breaks distal to the ITS are likely caused by incomplete replication of DNA distal to the ITS because of Rap1-mediated delay of fork progression at the ITS. Unexpectedly, we find that the GCR rate increases exponentially with ITS length (Fig. 1B and SI Appendix, Fig. S1). This suggests that Rap1 molecules are acting in a cooperative manner to obstruct DNA replication. The Rap1-interacting proteins Rif1 and Rif2 connect neighboring and distal DNA-bound Rap1 units to form a high-order interlinked scaffold (79),

the properties of which could change as telomere length increases. However, DNA-bound Rap1 obstructs replication independently of Rif1 and Rif2 (5, 14, 15). Rap1 has been reported to interact with DNA in multiple binding modes (80) and can, by itself, induce local DNA stiffening (81). Further studies are needed to determine whether these properties of Rap1 can explain why the GCR rate increases exponentially with telomere length.

Defects in DNA Replication Increase the ITS-Induced GCR Rate and Accelerate Replicative Senescence. We identified nine genes that suppress the ITS-induced GCR rate (Fig. 3C). Most have a direct function during DNA replication. If these mutants increase the GCR rate by increasing DNA breakage, they may also increase breaks at native telomeres that would accelerate senescence in the absence of telomerase. This is already known to be true for *cdc2-2* and *rad27Δ* (61, 62), and we show that *cdc2-7*, *cdc9-1*, *elg1Δ*, *rfc2-1*, and *rfc5-1* also do so, especially the latter two (Fig. 4). The dramatic effect of *rfc2-1* and *rfc5-1* on senescence is somewhat surprising given that they do not have the largest effects on the GCR rate, with or without an ITS present, and the *rfc4-20* mutant does not significantly affect senescence at all. However, analysis of the genetic interaction profile similarity subnetwork for the identified genes, extracted from the global network (82), reveals that *rfc2-1* and *rfc5-1*, while clustering among DNA replication and repair genes, are positioned further away than the other identified replication genes (SI Appendix, Fig. S5), indicating related but distinct functions. Consistent with this idea, Rfc2 and Rfc5 are unique among the small RFC subunits in that they are about twice as abundant as Rfc3 and Rfc4 (83), and can form a stable heterodimer that acts on PCNA in vitro (84). *rfc2-1 rfc5-1* double mutants are inviable, and overexpression of *RFC5* can suppress the temperature sensitivity of *rfc2-1* (85). Furthermore, the temperature sensitivity and replication defect of the *rfc5-1*

mutant can be suppressed by overexpression *POL30*, which encodes PCNA (86), suggesting that there is a deficiency in PCNA loading in this mutant. Thus, insufficient loading of PCNA may lead to replication defects that induce GCRs as well as accelerated senescence in the absence of telomerase.

It has been reported that the large subunit of RFC is aberrantly cleaved in Hutchinson–Gilford progeria syndrome (HGPS), resulting in defective loading of PCNA (87). HGPS is a disease characterized by accelerated aging and is caused by a mutation of the *LMNA* gene, leading to the expression of a truncated form of lamin A called progerin (88). At the cellular level, expression of progerin alters nuclear morphology and function, nucleolar activity, mitochondrial function, nucleocytoplasmic trafficking, and telomere homeostasis (89). It is still unclear how these alterations ultimately lead to the clinical features of HGPS, but telomere dysfunction may play a key role given that HGPS is associated with accelerated telomere erosion (90), and expression of telomerase improves the fitness of HGPS cells (91–93). Our findings support the hypothesis that premature senescence in HGPS is caused by a deficiency in PCNA loading and replication fork collapse at telomeres.

Interestingly, many of the other DNA replication genes identified in our screen have roles in lagging strand synthesis and Okazaki fragment processing. Elg1, in complex with Rfc2–5, unloads PCNA following Okazaki fragment ligation by Cdc9; depletion of Elg1 or Cdc9 causes accumulation of PCNA on DNA, which leads to genome instability (50, 94–97). Cells lacking Rad27 accumulate unligated Okazaki fragments (98), and presumably PCNA on DNA. Defects in lagging strand synthesis in the DNA polymerase δ mutants *cdc2-2* and *cdc2-7* would likely also increase the abundance of unligated Okazaki fragments and DNA-bound PCNA. Thus, a defect in unloading PCNA from DNA may also increase the probability of GCR.

The Presence of an ITS Heavily Biases Repair toward De Novo Telomere Addition. Surprisingly, our screen identified neither *PIF1* nor *RRM3*, which encode Pif1-family helicases. Stalling of replication forks traversing telomeric sequences increases in the absence of Rrm3, which is important for replication past nonhistone protein–DNA complexes (4, 99). Pif1 performs several functions that impact telomere biology, including inhibition of telomerase (100, 101), Okazaki fragment processing (102), unwinding of G-quadruplexes (103, 104), and promoting replication of Rap1-bound telomeric DNA (15, 21). Other genes encoding proteins known to suppress GCR in the absence of an ITS were also not identified, such as the MRX (Mre11–Rad50–Xrs2) complex, the STR (Sgs1–Top3–Rmi1) complex, the Mus81 endonuclease, and the SUMO-targeted ubiquitin ligase Slx5–Slx8. As they may have been false negatives in our screen, we tested deletions of some of these genes directly in the ITS–GCR assay.

Deletion of *PIF1*, which has been reported to cause an approximately 1,000-fold increase in the GCR rate in the absence of an ITS (67), only led to a 2.5-fold increase in the presence of a 50-bp ITS (Fig. 3D and *SI Appendix, Table S4*). We speculate that the role of Pif1 in suppressing GCR is primarily due to its function in suppressing de novo telomere addition (100), a function that is negated if the DNA end contains more than 34 bp of telomeric sequence (25). The residual 2.5-fold increase in the presence of the ITS could be due to the role of Pif1 in overcoming Rap1-dependent inhibition of DNA replication (15, 21), or its role in unwinding G-quadruplexes (103, 104). Consistent with that latter hypothesis, it has been previously reported that the GCR rate of the *pif1-m2* mutant, which is deficient in nuclear

Pif1, is increased threefold in the presence of G-quadruplex motif sequences (104).

Strains lacking any member of the MRX complex have an approximately 600-fold increase in the GCR rate in the absence of an ITS (22). Deletion of *SGS1* or *TOP3* increases the GCR rate by 20- to 30-fold, while deletion of *RM11* increases the GCR rate by more than 170-fold (46, 105, 106). Deletion of *MUS81* increases the GCR rate 100- to 200-fold, and deletion of *SLX5* or *SLX8* increases the GCR rate by more than 60-fold (46, 75, 107). We find that deletion of either *RAD50*, *SGS1*, *RM11*, *MUS81*, *SLX5*, or *SLX8* has a small or negligible effect on the GCR rate in the presence of a 50-bp ITS (Fig. 3D and *SI Appendix, Table S4*). The MRX and STR complexes are central players in the repair of DSBs (108, 109); Mus81 is a structure-specific endonuclease that resolves replication and recombination intermediates (110); Slx5–Slx8 plays diverse roles in genome maintenance (111). In the absence of an ITS, disruption of these complexes will increase the likelihood of inappropriate repair that leads to a GCR. This effect is likely negated when the DNA break occurs at or distally adjacent to an ITS since these breaks would be healed by de novo telomere addition regardless of whether these complexes are present. Consistent with this idea, a DSB that has telomeric repeats on one side of the DSB will result in asymmetric processing of the ends: The nontelomeric end will recruit the MRX complex and move to the nuclear pore complex while the telomeric side will not, favoring elongation by telomerase (112).

In summary, we have shown that ITSs are unstable and promote the formation of GCRs via multiple mechanisms. First, Rap1 impedes ITS replication, which increases the probability of fork collapse within the ITS. Second, impeding replication at the ITS will also increase fork collapse distal to the ITS due to incomplete replication of downstream DNA. Third, a DSB within or distal to the ITS, whether caused by fork collapse or other means, will bias repair toward de novo telomere addition, especially if at least 34 bp of telomere sequence remains on one side of the DSB. Last, transcription and NER can facilitate the formation of ITS-induced GCRs. Some of these mechanisms are also at play at native telomeres. For example, Rap1 also impedes replication at native telomeres, and a DSB within a telomere will be preferentially healed by telomerase, but this is not a problem precisely because it is desirable for a truncated telomere to be extended by telomerase. Thus, mechanisms that have evolved for proper telomere function are sources of instability and GCR at an ITS.

Materials and Methods

Yeast Strains and Media. All yeast strains used in this study are listed in *SI Appendix, Table S9*. To prevent the onset of replicative senescence, the est strains used in Fig. 5C were generated by replacing the corresponding *EST* gene with a kanMX cassette in ZYY141 and then used immediately for fluctuation tests without storing the strains. Standard yeast genetic and molecular methods were used (113, 114). Experiments involving a strain containing a ts allele were performed at 22 °C; in all other experiments, yeast strains were cultured at 30 °C. ITS and other DNA sequences were inserted in GCR assay-containing strains at the *PRB1* locus and are listed in *SI Appendix, Table S10*; the *hphMX* selection marker, which provides resistance to hygromycin B (115), was coinserted on the centromeric side of these DNA sequences.

Fluctuation Tests of GCR Rates. Fluctuation tests for the quantification of GCR rates were performed essentially as previously described (116) by transferring entire single colonies from YPD plates to 4 mL of YPD liquid medium. Cultures were grown to saturation (30 °C for YKO strains and 22 °C for ts mutants). 50 μ L of a 10^5 -fold dilution were plated in YPD plates. A strain-dependent quantity of cells was plated on SD-arg+canavanine+5-FOA. Colonies were counted after incubation at 30 °C or 22 °C for 3 to 7 d. The number of GCR (canavanine- and

5-FOA-resistant) colonies was used to calculate the GCR rate by the method of the median (117).

PCR and Sequencing of GCR Survivors. Genomic DNA from GCR survivors was isolated using a Wizard Genomic DNA Purification Kit (Promega). 1 μ L of genomic DNA (~100 ng) was mixed with 8 μ L of 1 \times Cutsmart buffer [New England Biolabs (NEB), Ipswich, MA] and boiled for 10 min at 94 $^{\circ}$ C. 1 μ L of tailing mix (0.05 μ L Terminal Transferase (NEB, cat. no. M0315), 0.1 μ L 10 \times Cutsmart buffer, 0.1 μ L 10 mM dCTP, 0.75 μ L dH₂O) was added and incubated for 30 min at 37 $^{\circ}$ C, 10 min at 65 $^{\circ}$ C, and 5 min at 96 $^{\circ}$ C. Immediately after tailing, 30 μ L of PCR mix was added. The PCR mix consisted of 4 μ L 10 \times PCR buffer [670 mM Tris-HCl pH 8.8, 160 mM (NH₄)₂SO₄, 50% glycerol, 0.1% Tween-20], 0.32 μ L 25 mM dNTP mix, 0.3 μ L 100 μ M site-specific primer (5'-TTTTCGCTCGACATCATCTGC-3'), 0.3 μ L 100 μ M G₁₈ primer (5'-CGGGATCCG₁₈-3'), 0.5 μ L Q5 High-Fidelity DNA Polymerase (NEB, cat. no. M0491), 24.68 μ L dH₂O. The samples were denatured at 98 $^{\circ}$ C for 3 min, followed by 35 cycles of 98 $^{\circ}$ C for 30 s, 68 $^{\circ}$ C for 15 s, and a final extension step at 72 $^{\circ}$ C for 2 min. PCR products were separated on 2.5% agarose gels and extracted using a NucleoSpin Gel and PCR Clean-up kit (Macherey-Nagel, Düren, Germany, cat. no. 740609). The purified PCR products were then cloned using a Zero Blunt TOPO PCR Cloning Kit (Thermo Fisher Scientific, cat. no. 450245). Individual clones were sequenced by Eurofins Genomics (Germany) and the resulting data were analyzed using Sequencher software (Gene Codes, Ann Arbor, MI).

Library Construction Using the Synthetic Genetic Array (SGA) Method. Strain FRY910 was used as the query strain to introduce *prb1 Δ hphMX-50bp_{-ITS}* and *hxt13 Δ URA3* into the YKO and ts libraries, with each strain in the libraries present in quadruplicate, using the SGA method (44) and a ROTOR-HDA pinning robot (Singer Instruments). The steps were performed at 30 $^{\circ}$ C and 22 $^{\circ}$ C for the YKO and ts strains, respectively. A few minor modifications to the SGA method were necessary. Standard SGA query strains contain the *can1 Δ ::P_{STE2}-Sp_{-his5}* cassette to allow selection of haploids. However, since *CAN1* is needed for the GCR assay, FRY910 contains the wild-type *CAN1* gene along with the *mfa1::P_{MFA1}-HIS3* cassette. After sporulation, cells were sequentially pinned onto synthetic (SD) medium lacking histidine and lysine, but containing thialysine (to select for *MATa* haploids), onto SD medium lacking histidine and lysine, but containing thialysine and G418 (to select for *MATa* haploids containing the YKO or ts allele), and finally onto SD medium lacking histidine, lysine, and uracil, but containing thialysine, G418, hygromycin B (to select for *MATa* haploids containing the YKO or ts allele, *prb1 Δ hphMX-50bp_{-ITS}*, and *hxt13 Δ URA3*). The resulting strains were then used in the genome-wide screens to identify mutants with an increased or decreased ITS-GCR rate.

Genome-Wide Screen for Mutants with an Increased ITS-GCR Rate. The high-throughput replica-pinning screen was performed essentially as previously described (41). In brief, YKO and ts strains containing *prb1 Δ hphMX-50bp_{-ITS}* and *hxt13 Δ URA3* were constructed with the SGA method (see above). The screen was performed at 30 $^{\circ}$ C and 22 $^{\circ}$ C for the YKO and ts strains, respectively. Strains in which less than two colonies (out of a possible four) grew on the final SGA plates were excluded from further analysis. Each (SD-histidine, lysine, uracil+thialysine, G418, hygromycin B) plate of the resulting quadruplicated *prb1 Δ hphMX-50bp_{-ITS}* *hxt13 Δ URA3 xxx::kanMX* strains (where xxx::kanMX indicates either a gene knockout or ts allele) was replica pinned twice in succession onto six SD-arginine+canavanine, 5-FOA plates, yielding 24 colonies per strain. Only hits with a Fisher's exact test *P*-value less than 0.002, comparing to the observed number of colonies on selective and nonselective plates for all strains in the screen, were selected for validation, which occurred in two steps. First, for only the screen hits, the *prb1 Δ hphMX-50bp_{-ITS}* *hxt13 Δ URA3 xxx::kanMX* strains were generated again by the SGA method. Each strain was then streaked in a 1 cm \times 1.5 cm patch on an SD-uracil plate, incubated at 30 $^{\circ}$ C (for YKO strains) or 22 $^{\circ}$ C (for ts strains) for 24 to 48 h, replica-plated on SD-arginine, canavanine, 5-FOA to detect GCR events, and scored by visual inspection. Twenty-one strains (5 YKO and 16 ts) passed this validation step. These YKO or ts mutants were tested with one fluctuation test, and if an increase in the ITS-GCR rate was observed, the mutants were introduced into a different strain background (W303), and then subsequently subjected to at least three additional fluctuation tests.

Rap1 Immunoblotting. Cells were harvested and fixed using 20% trichloroacetic acid (TCA). A FastPrep 5G system (MP Biomedicals) was employed for cell disruption, following the recommended program for *S. cerevisiae*. An additional 5% TCA was added to adjust the final TCA concentration to 7.3%. The samples were then centrifuged at 14,000 rpm for 10 min at 4 $^{\circ}$ C, after which the supernatant was discarded. Samples were resuspended in 1 \times loading buffer and loaded on 10% polyacrylamide gels. Proteins were transferred onto polyvinylidene difluoride membranes. The membranes were blocked in 2.5% bovine serum albumin (BSA) for 60 min at room temperature and incubated with Rap1 antibody (sc-374297; Santa Cruz Biotechnology) in 2.5% BSA overnight at 4 $^{\circ}$ C. The membranes were washed three times with 1 \times TBS containing 0.1% Tween 20 (Sigma) and incubated with m-IgG κ BP-HRP antibody (sc-516102; Santa Cruz Biotechnology) in 2.5% BSA for 2 h at room temperature. Blots were visualized using the Gel Doc XR+ System (Bio-Rad Laboratories).

Liquid Culture Senescence Assay. Liquid culture senescence assays were performed essentially as previously described (118). Each senescence assay started with diploid strains. Freshly dissected haploid spores were allowed to form colonies on YPD agar plates after 2 d of growth at 30 $^{\circ}$ C or 22 $^{\circ}$ C. Cells from these colonies were serially passaged in liquid culture medium at 24-h intervals. For each passage, the cell density of each culture was measured by optical density (calibrated by cell counting using a hemocytometer), and the cultures were diluted back into fresh medium at a cell density of 2 \times 10⁵ cells/mL. Cell density was plotted as a function of population doublings.

Genome-Wide Screen for Mutants with a Decreased ITS-GCR Rate. To screen for mutants with a decreased ITS-GCR rate, the high-throughput replica-pinning screen was repeated with a few modifications. In brief, the SGA-derived *prb1 Δ hphMX-50bp_{-ITS}* *hxt13 Δ URA3 xxx::kanMX* strains were replica pinned (from SD-histidine, lysine, uracil+thialysine, G418, hygromycin B) onto six YPD+ G418, hygromycin B, yielding 24 colonies per strain. The strains were then repinned twice in succession onto SD-arginine, canavanine, 5-FOA plates. Only hits with a Fisher's exact test *P*-value less than 10⁻⁴ were selected for validation. A lower *P*-value was used due to the higher number of hits. Validation occurred in several steps. First, for only the screen hits, the *prb1 Δ hphMX-50bp_{-ITS}* *hxt13 Δ URA3 xxx::kanMX* strains were generated again by the SGA method. Each strain was then streaked in a 1 cm \times 1.5 cm patch on an SD-uracil plate, incubated at 30 $^{\circ}$ C (for YKO strains) or 22 $^{\circ}$ C (for ts strains) for 24 to 48 h, replica-plated on SD-arginine, canavanine, 5-FOA to detect GCR events, and scored by visual inspection. Second, the strains were generated again by the SGA method, but with an extra copy of *CIN8* (*ho::CIN8-natMX*) also introduced into the YKO and ts strains. These strains were also tested using the patch-and-replica-plate approach. Third, a GCR survivor (ZYY261) was generating by growing FRY910 (the SGA starting strain with the 50-bp ITS and GCR markers) on media containing canavanine and 5-FOA. ZYY261 was confirmed by PCR and sequencing to have a de novo telomere added at the ITS site. ZYY261 was crossed to the hits from the screen using the SGA method, and resulting strains that showed a synthetic genetic growth defect by visual comparison of colony sizes were eliminated from further analysis. Last, due to the large number of hits that passed the first three validation steps, only a subset of these was subsequently subjected to at least three fluctuation tests, and the mutants were not tested in a different strain background.

Gene Ontology Enrichment Analysis. The GO term finder tool (<http://go.princeton.edu/>) was used to query biological process enrichment for each gene set, with a *P*-value cutoff of 0.01 and Bonferroni correction applied. REVIGO (119) was used to further analyze the GO term enrichment data, using the "Medium (0.7)" term similarity filter and the simRel score as semantic similarity measure. As a result, terms with a frequency more than 10% in the REVIGO output were eliminated for being too broad.

Data, Materials, and Software Availability. All study data are included in the article and/or [supporting information](#).

ACKNOWLEDGMENTS. We thank G.W. Brown for providing yeast strains; B. Luke for providing plasmids pBL190, pBL192, and pBL710; and D. Novarina and L.M. Veenhoff for critical reading of the manuscript. F.R.R.B. was supported

by a Consejo Nacional de Ciencia y Tecnología scholarship. Z.Y. was supported by a scholarship from the Nanjing Huimou Medi-Tech Co. Y.Y. was supported by scholarships from the University of Groningen's Abel Tasman Talent and from

the Chongqing Explorer Decoration Engineering Co. Work in the laboratory of M.C. was supported by an Open Competition M-2 grant from the Dutch Research Council.

1. D. Jain, J. P. Cooper, Telomeric strategies: Means to an end. *Annu. Rev. Genet.* **44**, 243-269 (2010).
2. R. J. Wellinger, In the end, what's the problem? *Mol. Cell* **53**, 855-856 (2014).
3. E. H. Blackburn, K. Collins, Telomerase: An RNP enzyme synthesizes DNA. *Cold Spring Harb. Perspect. Biol.* **3**, a003558 (2011).
4. A. S. Ivessa, J. Q. Zhou, V. P. Schulz, E. K. Monson, V. A. Zakian, *Saccharomyces Rrm3p*, a 5' to 3' DNA helicase that promotes replication fork progression through telomeric and subtelomeric DNA. *Genes Dev.* **16**, 1383-1396 (2002).
5. S. Makovets, I. Herskowitz, E. H. Blackburn, Anatomy and dynamics of DNA replication fork movement in yeast telomeric regions. *Mol. Cell Biol.* **24**, 4019-4031 (2004).
6. K. M. Miller, O. Rog, J. P. Cooper, Semi-conservative DNA replication through telomeres requires Taz1. *Nature* **440**, 824-828 (2006).
7. A. Sfeir *et al.*, Mammalian telomeres resemble fragile sites and require TRF1 for efficient replication. *Cell* **138**, 90-103 (2009).
8. M. L. Bochman, K. Paeschke, V. A. Zakian, DNA secondary structures: Stability and function of G-quadruplex structures. *Nat. Rev. Genet.* **13**, 770-780 (2012).
9. J. Rivosecchi, K. Jurikova, E. Cusanelli, Telomere-specific regulation of TERRA and its impact on telomere stability. *Semin. Cell Dev. Biol.* **157**, 3-23 (2024).
10. A. Ruiz-Herrera, S. G. Nergadze, M. Santagostino, E. Giulotto, Telomeric repeats far from the ends: Mechanisms of origin and role in evolution. *Cytogenet. Genome Res.* **122**, 219-228 (2008).
11. A. Y. Aksenova, S. M. Mirkin, At the beginning of the end and in the middle of the beginning: Structure and maintenance of telomeric DNA repeats and interstitial telomeric sequences. *Genes (Basel)* **10**, 118 (2019).
12. S. G. Nergadze, M. A. Santagostino, A. Salzano, C. Mondello, E. Giulotto, Contribution of telomerase RNA retrotranscription to DNA double-strand break repair during mammalian genome evolution. *Genome Biol.* **8**, R260 (2007).
13. R. P. Anand *et al.*, Overcoming natural replication barriers: Differential helicase requirements. *Nucleic Acids Res.* **40**, 1091-1105 (2012).
14. G. H. Goto *et al.*, Binding of multiple Rap1 proteins stimulates chromosome breakage induction during DNA replication. *PLoS Genet.* **11**, e1005283 (2015).
15. M. E. Douglas, J. F. X. Diffley, Budding yeast Rap1, but not telomeric DNA, is inhibitory for multiple stages of DNA replication in vitro. *Nucleic Acids Res.* **49**, 5671-5683 (2021).
16. A. Ruiz-Herrera *et al.*, Evolutionary breakpoints are co-localized with fragile sites and intrachromosomal telomeric sequences in primates. *Cytogenet. Genome Res.* **108**, 234-247 (2005).
17. A. Y. Aksenova *et al.*, Genome rearrangements caused by interstitial telomeric sequences in yeast. *Proc. Natl. Acad. Sci. U.S.A.* **110**, 19866-19871 (2013).
18. A. O. Wilkie, J. Lamb, P. C. Harris, R. D. Finney, D. R. Higgs, A truncated human chromosome 16 associated with α -thalassaemia is stabilized by addition of telomeric repeat (TTAGGG)_n. *Nature* **346**, 868-871 (1990).
19. J. Lamb *et al.*, De novo truncation of chromosome 16p and healing with (TTAGGG)_n in the α -thalassaemia/mental retardation syndrome (ATR-16). *Am. J. Hum. Genet.* **52**, 668-676 (1993).
20. A. C. Wong *et al.*, Molecular characterization of a 130-kb terminal microdeletion at 22q in a child with mild mental retardation. *Am. J. Hum. Genet.* **60**, 113-120 (1997).
21. K. N. Koc, S. P. Singh, J. L. Stodola, P. M. Burgers, R. Galletto, Pif1 removes a Rap1-dependent barrier to the strand displacement activity of DNA polymerase delta. *Nucleic Acids Res.* **44**, 3811-3819 (2016).
22. C. Chen, R. D. Kolodner, Gross chromosomal rearrangements in *Saccharomyces cerevisiae* replication and recombination defective mutants. *Nat. Genet.* **23**, 81-85 (1999).
23. D. E. Gottschling, O. M. Aparicio, B. L. Billington, V. A. Zakian, Position effect at *S. cerevisiae* telomeres: Reversible repression of Pol II transcription. *Cell* **63**, 751-762 (1990).
24. O. M. Aparicio, B. L. Billington, D. E. Gottschling, Modifiers of position effect are shared between telomeric and silent mating-type loci in *S. cerevisiae*. *Cell* **66**, 1279-1287 (1991).
25. J. Strecker *et al.*, A sharp Pif1-dependent threshold separates DNA double-strand breaks from critically short telomeres. *Elife* **6**, e23783 (2017).
26. M. Chang, M. Arneric, J. Lingner, Telomerase repeat addition processivity is increased at critically short telomeres in a Tel1-dependent manner in *Saccharomyces cerevisiae*. *Genes Dev.* **21**, 2485-2494 (2007).
27. K. Förstemann, J. Lingner, Molecular basis for telomere repeat divergence in budding yeast. *Mol. Cell Biol.* **21**, 7277-7286 (2001).
28. F. R. Rosas Bringas, S. Stinus, P. de Zoeten, M. Cohn, M. Chang, Rif2 protects Rap1-depleted telomeres from MRX-mediated degradation in *Saccharomyces cerevisiae*. *Elife* **11**, e74090 (2022).
29. I. R. Graham, A. Chambers, Use of a selection technique to identify the diversity of binding sites for the yeast RAP1 transcription factor. *Nucleic Acids Res.* **22**, 124-130 (1994).
30. S. Stinus, F. R. Rosas Bringas, L. Wanders, M. Chang, Investigating the role of G-quadruplexes at *Saccharomyces cerevisiae* telomeres. *Microbial. Cell* **9**, 126-132 (2022).
31. J. Shampay, J. W. Szostak, E. H. Blackburn, DNA sequences of telomeres maintained in yeast. *Nature* **310**, 154-157 (1984).
32. J. R. Williamson, M. K. Raghuraman, T. R. Cech, Monovalent cation-induced structure of telomeric DNA: The G-quartet model. *Cell* **59**, 871-880 (1989).
33. J. Berman, C. Y. Tachibana, B. K. Tye, Identification of a telomere-binding activity from yeast. *Proc. Natl. Acad. Sci. U.S.A.* **83**, 3713-3717 (1986).
34. A. N. Khristich, S. M. Mirkin, On the wrong DNA track: Molecular mechanisms of repeat-mediated genome instability. *J. Biol. Chem.* **295**, 4134-4170 (2020).
35. K. T. Xie *et al.*, DNA fragility in the parallel evolution of pelvic reduction in stickleback fish. *Science* **363**, 81-84 (2019).
36. K. Myung, A. Datta, R. D. Kolodner, Suppression of spontaneous chromosomal rearrangements by S phase checkpoint functions in *Saccharomyces cerevisiae*. *Cell* **104**, 397-408 (2001).
37. U. C. Obodo *et al.*, Endogenous hotspots of *de novo* telomere addition in the yeast genome contain proximal enhancers that bind Cdc13. *Mol. Cell Biol.* **36**, 1750-1763 (2016), 10.1128/mcb.00095-16.
38. B. Garvik, M. Carson, L. Hartwell, Single-stranded DNA arising at telomeres in *cdc13* mutants may constitute a specific signal for the *RAD9* checkpoint. *Mol. Cell Biol.* **15**, 6128-6138 (1995).
39. H. P. Ngo, D. Lydall, Survival and growth of yeast without telomere capping by Cdc13 in the absence of Sgs1, Exo1, and Rad9. *PLoS Genet.* **6**, e1001072 (2010).
40. A. Y. Aksenova, G. Han, A. A. Shishkin, K. V. Volkov, S. M. Mirkin, Expansion of interstitial telomeric sequences in yeast. *Cell Rep.* **13**, 1545-1551 (2015).
41. D. Novarina, F. R. Rosas Bringas, O. G. Rosas Bringas, M. Chang, High-throughput replica-pinning approach to screen for yeast genes controlling low-frequency events. *STAR Protoc.* **3**, 101082 (2022).
42. G. Gaever *et al.*, Functional profiling of the *Saccharomyces cerevisiae* genome. *Nature* **418**, 387-391 (2002).
43. Z. Li *et al.*, Systematic exploration of essential yeast gene function with temperature-sensitive mutants. *Nat. Biotechnol.* **29**, 361-367 (2011).
44. E. Kuzmin, M. Costanzo, B. Andrews, C. Boone, Synthetic genetic array analysis. *Cold Spring Harb. Protoc.* 2016, pdb prot088807 (2016).
45. M. Chang, A. B. Parsons, B. H. Sheikh, C. Boone, G. W. Brown, Genomic approaches for identifying DNA damage response pathways in *S. cerevisiae*. *Methods Enzymol.* **409**, 213-235 (2006).
46. C. D. Putnam *et al.*, Bioinformatic identification of genes suppressing genome instability. *Proc. Natl. Acad. Sci. U.S.A.* **109**, E3251-E3259 (2012).
47. K. C. Sitney, M. E. Budd, J. L. Campbell, DNA polymerase III, a second essential DNA polymerase, is encoded by the *S. cerevisiae CDC2* gene. *Cell* **56**, 599-605 (1989).
48. A. Boulet, M. Simon, G. Faye, G. A. Bauer, P. M. Burgers, Structure and function of the *Saccharomyces cerevisiae CDC2* gene encoding the large subunit of DNA polymerase III. *EMBO J.* **8**, 1849-1854 (1989).
49. N. Y. Yao, M. O'Donnell, The RFC clamp loader: Structure and function. *Subcell Biochem.* **62**, 259-279 (2012).
50. T. Kubota, K. Nishimura, M. T. Kanemaki, A. D. Donaldson, The Elg1 replication factor C-like complex functions in PCNA unloading during DNA replication. *Mol. Cell* **50**, 273-280 (2013).
51. Y. Liu, H. I. Kao, R. A. Bambara, Flap endonuclease 1: A central component of DNA metabolism. *Annu. Rev. Biochem.* **73**, 589-615 (2004).
52. L. H. Johnston, K. A. Nasmyth, *Saccharomyces cerevisiae* cell cycle mutant *cdc9* is defective in DNA ligase. *Nature* **274**, 891-893 (1978).
53. X. Pan *et al.*, A DNA integrity network in the yeast *Saccharomyces cerevisiae*. *Cell* **124**, 1069-1081 (2006).
54. H. B. McDonald, A. H. Helfant, E. M. Mahony, S. K. Khosla, L. Goetsch, Mutational analysis reveals a role for the C terminus of the proteasome subunit Rpt4p in spindle pole body duplication in *Saccharomyces cerevisiae*. *Genetics* **162**, 705-720 (2002).
55. J. J. Morgan, L. J. Crawford, The ubiquitin proteasome system in genome stability and cancer. *Cancers (Basel)* **13**, 2235 (2021).
56. C. D. Putnam, R. D. Kolodner, Pathways and mechanisms that prevent genome instability in *Saccharomyces cerevisiae*. *Genetics* **206**, 1187-1225 (2017).
57. K. H. Schmidt, R. D. Kolodner, Suppression of spontaneous genome rearrangements in yeast DNA helicase mutants. *Proc. Natl. Acad. Sci. U.S.A.* **103**, 18196-18201 (2006).
58. L. S. Symington, R. Rothstein, M. Lisby, Mechanisms and regulation of mitotic recombination in *Saccharomyces cerevisiae*. *Genetics* **198**, 795-835 (2014).
59. A. Lengronne, E. Schwob, The yeast CDK inhibitor Sic1 prevents genomic instability by promoting replication origin licensing in late G1. *Mol. Cell* **9**, 1067-1078 (2002).
60. P. Ayuda-Duran *et al.*, The CDK regulators Cdh1 and Sic1 promote efficient usage of DNA replication origins to prevent chromosomal instability at a chromosome arm. *Nucleic Acids Res.* **42**, 7057-7068 (2014).
61. Y. L. Tsai, S. F. Tseng, S. H. Chang, C. C. Lin, S. C. Teng, Involvement of replicative polymerases, Tel1p, Mec1p, Cdc13p, and the Ku complex in telomere-telomere recombination. *Mol. Cell Biol.* **22**, 5679-5687 (2002).
62. J. Parenteau, R. J. Wellinger, Differential processing of leading- and lagging-strand ends at *Saccharomyces cerevisiae* telomeres revealed by the absence of Rad27p nuclease. *Genetics* **162**, 1583-1594 (2002).
63. J. Lingner *et al.*, Reverse transcriptase motifs in the catalytic subunit of telomerase. *Science* **276**, 561-567 (1997).
64. T. S. Lendvay, D. K. Morris, J. Sah, B. Balasubramanian, V. Lundblad, Senescence mutants of *Saccharomyces cerevisiae* with a defect in telomere replication identify three additional *EST* genes. *Genetics* **144**, 1399-1412 (1996).
65. Y. Yao *et al.*, Revisiting the role of the spindle assembly checkpoint in the formation of gross chromosomal rearrangements in *Saccharomyces cerevisiae*. *Genetics* **228**, iyae150 (2024), 10.1093/genetics/iyae150.
66. R. J. Wellinger, V. A. Zakian, Everything you ever wanted to know about *Saccharomyces cerevisiae* telomeres: Beginning to end. *Genetics* **191**, 1073-1105 (2012).
67. K. Myung, C. Chen, R. D. Kolodner, Multiple pathways cooperate in the suppression of genome instability in *Saccharomyces cerevisiae*. *Nature* **411**, 1073-1076 (2001).
68. C. I. Nugent, T. R. Hughes, N. F. Lue, V. Lundblad, Cdc13p: A single-strand telomeric DNA-binding protein with a dual role in yeast telomere maintenance. *Science* **274**, 249-252 (1996).
69. W. H. Chung, Z. Zhu, A. Papusha, A. Malkova, G. Ira, Defective resection at DNA double-strand breaks leads to *de novo* telomere formation and enhances gene targeting. *PLoS Genet.* **6**, 24 (2010).
70. S. Kurtz, D. Shore, RAP1 protein activates and silences transcription of mating-type genes in yeast. *Genes Dev.* **5**, 616-628 (1991).
71. G. Kyriou, K. A. Boakye, A. J. Lustig, C-terminal truncation of RAP1 results in the deregulation of telomere size, stability, and function in *Saccharomyces cerevisiae*. *Mol. Cell Biol.* **12**, 5159-5173 (1992).
72. C. F. Hardy, L. Sussel, D. Shore, A RAP1-interacting protein involved in transcriptional silencing and telomere length regulation. *Genes Dev.* **6**, 801-814 (1992).
73. D. Wolton, D. Shore, A novel Rap1p-interacting factor, Rif2p, cooperates with Rif1p to regulate telomere length in *Saccharomyces cerevisiae*. *Genes Dev.* **11**, 748-760 (1997).
74. P. Moretti, K. Freeman, L. Coadly, D. Shore, Evidence that a complex of SIR proteins interacts with the silencer and telomere-binding protein RAP1. *Genes Dev.* **8**, 2257-2269 (1994).

75. J. Y. Hwang, S. Smith, K. Myung, The Rad1–Rad10 complex promotes the production of gross chromosomal rearrangements from spontaneous DNA damage in *Saccharomyces cerevisiae*. *Genetics* **169**, 1927–1937 (2005).
76. A. J. Bardwell, L. Bardwell, A. E. Tomkinson, E. C. Friedberg, Specific cleavage of model recombination and repair intermediates by the yeast Rad1–Rad10 DNA endonuclease. *Science* **265**, 2082–2085 (1994).
77. S. Boiteux, S. Jinks–Robertson, DNA repair mechanisms and the bypass of DNA damage in *Saccharomyces cerevisiae*. *Genetics* **193**, 1025–1064 (2013).
78. J. Sollier *et al.*, Transcription-coupled nucleotide excision repair factors promote R-loop-induced genome instability. *Mol. Cell* **56**, 777–785 (2014).
79. T. Shi *et al.*, Rif1 and Rif2 shape telomere function and architecture through multivalent Rap1 interactions. *Cell* **153**, 1340–1353 (2013).
80. E. A. Feldmann, R. Galletto, The DNA-binding domain of yeast Rap1 interacts with double-stranded DNA in multiple binding modes. *Biochemistry* **53**, 7471–7483 (2014).
81. Y. V. Le Bihan *et al.*, Effect of Rap1 binding on DNA distortion and potassium permanganate hypersensitivity. *Acta Crystallogr. D Biol. Crystallogr.* **69**, 409–419 (2013).
82. M. Costanzo *et al.*, A global genetic interaction network maps a wiring diagram of cellular function. *Science* **353**, aaf1420 (2016).
83. S. Ghaemmaghami *et al.*, Global analysis of protein expression in yeast. *Nature* **425**, 737–741 (2003).
84. N. Y. Yao, A. Johnson, G. D. Bowman, J. Kuriyan, M. O'Donnell, Mechanism of proliferating cell nuclear antigen clamp opening by replication factor C. *J. Biol. Chem.* **281**, 17528–17539 (2006).
85. V. N. Noskov, H. Araki, A. Sugino, The *RFC2* gene, encoding the third-largest subunit of the replication factor C complex, is required for an S-phase checkpoint in *Saccharomyces cerevisiae*. *Mol. Cell Biol.* **18**, 4914–4923 (1998).
86. K. Sugimoto *et al.*, Rfc5, a small subunit of replication factor C complex, couples DNA replication and mitosis in budding yeast. *Proc. Natl. Acad. Sci. U.S.A.* **93**, 7048–7052 (1996).
87. H. Tang, B. Hilton, P. R. Musich, D. Z. Fang, Y. Zou, Replication factor C1, the large subunit of replication factor C, is proteolytically truncated in Hutchinson–Gilford progeria syndrome. *Aging Cell* **11**, 363–365 (2012).
88. M. Eriksson *et al.*, Recurrent de novo point mutations in lamin A cause Hutchinson–Gilford progeria syndrome. *Nature* **423**, 293–298 (2003).
89. B. Cisneros, I. Garcia–Aguirre, M. De Ita, I. Arrieta–Cruz, H. Rosas–Vargas, Hutchinson–Gilford progeria syndrome: Cellular mechanisms and therapeutic perspectives. *Arch. Med. Res.* **54**, 102837 (2023).
90. M. L. Decker, E. Chavez, I. Vulto, P. M. Lansdorp, Telomere length in Hutchinson–Gilford progeria syndrome. *Mech. Ageing Dev.* **130**, 377–383 (2009).
91. B. A. Kudlow, M. N. Stanfel, C. R. Burtner, E. D. Johnston, B. K. Kennedy, Suppression of proliferative defects associated with processing-defective lamin A mutants by hTERT or inactivation of p53. *Mol. Biol. Cell* **19**, 5238–5248 (2008).
92. E. K. Benson, S. W. Lee, S. A. Aaronson, Role of progerin-induced telomere dysfunction in HGPS premature cellular senescence. *J. Cell Sci.* **123**, 2605–2612 (2010).
93. Y. Li *et al.*, Transient introduction of human telomerase mRNA improves hallmarks of progeria cells. *Aging Cell* **18**, e12979 (2019).
94. T. Kubota, Y. Katou, R. Nakato, K. Shirahige, A. D. Donaldson, Replication-coupled PCNA unloading by the Elg1 complex occurs genome-wide and requires Okazaki fragment ligation. *Cell Rep.* **12**, 774–787 (2015).
95. C. Yu *et al.*, Strand-specific analysis shows protein binding at replication forks and PCNA unloading from lagging strands when forks stall. *Mol. Cell* **56**, 551–563 (2014).
96. C. Johnson, V. K. Gali, T. S. Takahashi, T. Kubota, PCNA retention on DNA into G2/M phase causes genome instability in cells lacking Elg1. *Cell Rep.* **16**, 684–695 (2016).
97. K. Shemesh *et al.*, A structure-function analysis of the yeast Elg1 protein reveals the importance of PCNA unloading in genome stability maintenance. *Nucleic Acids Res.* **45**, 3189–3203 (2017).
98. B. J. Merrill, C. Holm, The *RAD52* recombinational repair pathway is essential in *pol30* (PCNA) mutants that accumulate small single-stranded DNA fragments during DNA synthesis. *Genetics* **148**, 611–624 (1998).
99. A. S. Ivesa *et al.*, The *Saccharomyces cerevisiae* helicase Rrm3p facilitates replication past nonhistone protein–DNA complexes. *Mol. Cell* **12**, 1525–1536 (2003).
100. V. P. Schulz, V. A. Zakian, The *Saccharomyces PIF1* DNA helicase inhibits telomere elongation and de novo telomere formation. *Cell* **76**, 145–155 (1994).
101. J. B. Boulé, L. R. Vega, V. A. Zakian, The yeast Pif1p helicase removes telomerase from telomeric DNA. *Nature* **438**, 57–61 (2005).
102. M. E. Budd, C. C. Reis, S. Smith, K. Myung, J. L. Campbell, Evidence suggesting that Pif1 helicase functions in DNA replication with the Dna2 helicase/nuclease and DNA polymerase delta. *Mol. Cell Biol.* **26**, 2490–2500 (2006).
103. K. Paeschke, J. A. Capra, V. A. Zakian, DNA replication through G-quadruplex motifs is promoted by the *Saccharomyces cerevisiae* Pif1 DNA helicase. *Cell* **145**, 678–691 (2011).
104. K. Paeschke *et al.*, Pif1 family helicases suppress genome instability at G-quadruplex motifs. *Nature* **497**, 458–462 (2013).
105. K. Myung, A. Datta, C. Chen, R. D. Kolodner, SGS1, the *Saccharomyces cerevisiae* homologue of BLM and WRN, suppresses genome instability and homeologous recombination. *Nat. Genet.* **27**, 113–116 (2001).
106. M. Chang *et al.*, *RMI1/NCE4*, a suppressor of genome instability, encodes a member of the RecQ helicase/Topo III complex. *EMBO J.* **24**, 2024–2033 (2005).
107. C. Zhang, T. M. Roberts, J. Yang, R. Desai, G. W. Brown, Suppression of genomic instability by *SLX5* and *SLX8* in *Saccharomyces cerevisiae*. *DNA Repair* **5**, 336–346 (2006).
108. J. Oh, L. S. Symington, Role of the Mre11 complex in preserving genome integrity. *Genes (Basel)* **9**, 589 (2018).
109. K. A. Bernstein, S. Gangloff, R. Rothstein, The RecQ DNA helicases in DNA repair. *Annu. Rev. Genet.* **44**, 393–417 (2010).
110. B. Pfander, J. Matos, Control of Mus81 nuclease during the cell cycle. *FEBS Lett.* **591**, 2048–2056 (2017).
111. Y. C. Chang, M. K. Oram, A. K. Bielinsky, SUMO-targeted ubiquitin ligases and their functions in maintaining genome stability. *Int. J. Mol. Sci.* **22**, 5391 (2021).
112. I. Marcomini *et al.*, Asymmetric processing of DNA ends at a double-strand break leads to unconstrained dynamics and ectopic translocation. *Cell Rep.* **24**, 2614–2628.e4 (2018).
113. F. Sherman, Getting started with yeast. *Methods Enzymol.* **350**, 3–41 (2002).
114. D. C. Amberg, D. Burke, J. N. Strathern, *Methods in Yeast Genetics: A Cold Spring Harbor Laboratory Course Manual* (Cold Spring Harbor Laboratory Press, Cold Spring Harbor, NY, 2005).
115. A. L. Goldstein, J. H. McCusker, Three new dominant drug resistance cassettes for gene disruption in *Saccharomyces cerevisiae*. *Yeast* **15**, 1541–1553 (1999).
116. C. D. Putnam, R. D. Kolodner, Determination of gross chromosomal rearrangement rates. *Cold Spring Harb. Protoc.* 2010, pdb prot5492 (2010).
117. D. E. Lea, C. A. Coulson, The distribution of the numbers of mutants in bacterial populations. *J. Genet.* **49**, 264–285 (1949).
118. P. M. van Mourik *et al.*, Recombination-mediated telomere maintenance in *Saccharomyces cerevisiae* is not dependent on the Shu complex. *PLoS One* **11**, e0151314 (2016).
119. F. Supek, M. Bosnjak, N. Skunca, T. Smuc, REVIGO summarizes and visualizes long lists of gene ontology terms. *PLoS One* **6**, e21800 (2011).